Design Optimization of PM Synchronous Motor Used in Belt Drive Elevator Systems

Yusuf Avsar
Department of Electronics and Automation
Trakya University
Edirne, Turkey
yusufavsar@trakya.edu.tr

Ahmet Fenercioglu
Department of Mechatronics Engineering
Tokat Gaziosmanpasa University
Tokat, Turkey
ahmet.fenercioglu@gop.edu.tr

Mucahit Soyaslan
Department of Mechatronics Engineering
Sakarya University of Applied Sciences
Sakarya, Turkey
msoyaslan@subu.edu.tr

***Abstract* — In this paper, the design and optimization of 4.5 kW inner rotor permanent magnet synchronous motor (PMSM) with 400 rpm nominal speed was carried out for belt drive elevator systems. The two most important criteria to be considered in elevator traction motors are to provide high efficiency and passenger comfort. For this reason, a design with a minimum torque ripple was aimed in the IE4 class. Electrical and magnetic modelling of PMSM has been carried out. Based on the acquired limit values and using the 2D finite element method (FEM), the optimization of parameters such as the slot opening (*Bs0*), magnet thickness (*Hmag*), embrace (*Em*), stator tooth thickness (*Wth*) and air gap (*g*) was made via genetic algorithm. 18-slot 20-pole PMSM with a torque ripple of 0.37 (SI) and 90.63% efficiency was obtained according to optimization results.**

Keywords — PM synchronous motor, inner rotor, optimization, embrace, elevator traction machine, efficiency, gearless motor, genetic algorithm.

I. INTRODUCTION

Nowadays, the increasing need for housing and the housing projects which are carried out based on that need have accelerated the production of elevator systems. With the implementation of urban transformation projects in recent years, important developments have been taking place in the industry. Energy efficiency comes to the fore in the installed elevator systems. One of the most important parameters affecting energy efficiency in elevator systems is the traction motor [1]. If permanent magnet synchronous motors without gears are used instead of induction motors with gears, energy about 30-50% can be saved [2, 3]. This situation increases the usage rate of gearless PMSMs in the industry day by day.

In gearless elevator motors, elevator car and counterweight are moved by ropes or belts attached to pulleys. In order to prevent fractures that may occur in steel ropes, it is mandatory to provide a ratio of 40: 1 between the drive pulley and the rope diameter [4]. As a result of current risk analysis today, the smallest pulley diameter that can be used is 240 mm. Therefore, these diameters have made it necessary to obtain higher rated torques at lower speeds in direct drive gearless elevator motors. In order to move the same loads with low torques at high speeds, the pulley diameters must be more reduced. For this purpose, belt mechanisms have been used instead of the rope mechanisms in recent years [5]. As a result of the commercialization of suitable and certified belts made of steel core and rubber material, the fracture faults in the ropes were eliminated and the pulley diameters were able to be reduced to lower values. Thus, the motor dimensions that can move the same loads have also been reduced. With belt drive elevators, diameters of traction pulleys have decreased, smoother and quieter travels have been achieved and energy efficiency has increased much more [1].

Energy efficiencies in electric motors are classified from IE1 to IE5. At least IE3 motor efficiency is generally a mandatory standard and these standards vary according to the power value and pole numbers of the motors. In optimization studies with genetic algorithms; motor efficiency, electromagnetic performance, thermal performance and material costs were chosen as single and multiple objective functions [6, 7]. In this study; design and optimization of a belt-driven PMSM with 4.5 kW power, 1 m/s car speed, IE4 efficiency class, 630 kg load (8-person) was made. The basic design modeling of PMSM was carried out with analytical equations. The objective function has been chosen as the highest motor efficiency and minimum torque ripple. The optimization of the parameters directly affecting the slot opening (*Bs0*), magnet thickness (*Hmag*), embrace (*Em*), stator tooth thickness (*Wth*) and air gap (*g*) was carried out by using 2D FEM with genetic algorithm method.

II. INNER ROTOR PMSM DESIGN

Since the discovery of rare earth elements with high energy density, that is, after the 1970s, PMSMs with high power density have started to be produced [8]. Instead of low efficiency induction motors, PM synchronous motors have been used for a while in gearless elevator traction systems. While some of these motors are external rotor, most of them have inner rotor structure [9]. In this study, firstly analytical model of an inner rotor PMSM was obtained, and then optimization of selected parameters was performed according to efficiency and torque ripple objective functions.

A. Equivalent Circuit of PMSM

The magnetic equivalent circuit of PMSM is shown in Fig. 1. Since permanent magnets create flux in themselves, they are modeled as a flux source and indicated by ϕ_r. The magnet reluctance R_m is shown with the attention to magnetic polarity.

While some of the flux reaches the other pole through the air gap, the remaining flux reaches the other pole through the stator. The steel parts of the rotor and stator are respectively shown as R_r and R_s. The air gap reluctance is shown as R_g. The leakage flux resistance flowing from one magnet to another is R_l. The magnet flux is ϕ, the air gap flux ϕ_g, and the leakage flux is ϕ_l. According to the

978-1-7281-9951-1/21/$31.00 ©2021 IEEE

magnetic equivalent circuit, equations of critical values are shown in between (1-10) [10].

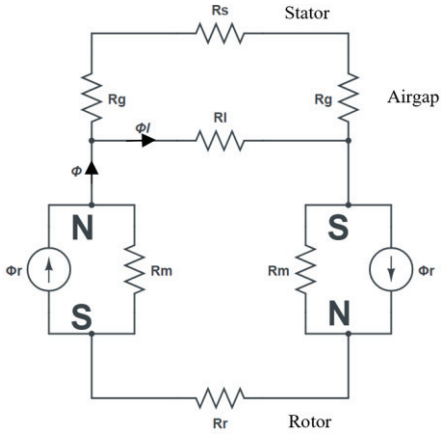

Fig. 1. The Magnetic equivalent circuit of PMSM [8]

Air gap flux can be shown as in (1). K_l in the equation is the leakage factor and its value is less than 1. K_r is the reluctance factor that slowly increases the air gap reluctance to regulate stray iron losses. These values are difficult to find with analytical methods and are generally determined according to the experience of the designer. Magnetic flux ϕ in Fig. 1 can be written as in (2).

$$\phi_g = K_l * \phi_r \tag{1}$$

$$\phi = \frac{2R_m}{2R_m+2K_rR_g}\phi_r = \frac{1}{1+K_r\frac{R_g}{R_m}}\phi_r \tag{2}$$

The magnet and air gap reluctances R_m and R_g are shown in (3) and (4) respectively [11]. The l_m value in these equations denotes the magnet length and the A_{mag} value denotes the magnet cross-sectional area. Likewise, g refers to the air gap length and A_g refers to the cross-sectional area.

$$R_m = \frac{l_m}{\mu_R\mu_0 A_{mag}} \tag{3}$$

$$R_g = \frac{g}{\mu_0 A_g} \tag{4}$$

Air gap flux can be written as in (5) according to the above equations.

$$\phi_g = K_l\phi = \frac{K_l}{1+K_r\frac{\mu_R g A_{mag}}{l_m A_g}}\phi_r \tag{5}$$

Flux concentration factor is shown in (6), and magnet flux density is shown in (7).

$$C_\emptyset = \frac{A_{mag}}{A_g} \tag{6}$$

$$B_r = \frac{\emptyset_r}{A_{mag}} \tag{7}$$

Air gap mangetic flux density is obtained by (8), and the permeance coefficient is obtained by (9).

$$B_g = \frac{\emptyset_g}{A_g} \tag{8}$$

$$P_c = \frac{l_m}{gC_\emptyset} \tag{9}$$

If all equations are arranged, the air gap flux density B_g can be written as in (10) [11].

$$B_g = \frac{K_lC_\emptyset}{1+K_r\frac{\mu_R}{P_c}}B_r \tag{10}$$

If PMSM will be designed according to the flux density in (10); the K_l leakage factor can be taken as between 0.9 and 1.0, the K_r reluctance factor can be taken between 1 and 1.2, and the flux concentration factor $C_\emptyset$ can be taken as 1. In this case, the only parameter can be changed will be the magnetic permeance coefficient P_c. That is, the thickness of the magnets and the air gap plays an important role in the motor design phase [12].

B. Back Electromotive Force (EMF)

The back EMF voltage generated in PMSMs contains a lot of information about the identification of the motor such as motor constant, number of poles, speed range, torque-speed characteristic, bus voltage, current waveform. Therefore, if the back EMF is expressed analytically, the analytical model of the motor can be easily derived [11]. For a PMSM with sinusoidal flux distribution, the expression for the back EMF voltage including the k_{sf} stacking factor and k_w winding factor is shared in (11) (The voltage in this equation is the peak value of the back emf). The stacking factor k_{sf} was taken as 0.95. This factor should be used while reaching the desired stack size, due to the gaps between the sheet metals [1]. The winding factor k_w was taken as 0.945 for designed motor with 18/20 slot-pole ratio.

$$\hat{E}_z = \frac{p}{2}\,\omega_m N_t \phi_g k_{sf} k_w \tag{11}$$

p in (11) represents the number of poles, ω_m represents the angular velocity of shaft in rad/s, N_t represents the total number of turns in a phase, ϕ_g represents the air gap flux as stated before. It is known that the expression of ϕ_g air gap flux is equal to the product of the average air gap flux density ($\bar{B}_g$) and the air gap cross-sectional area (A_g). The back EMF voltage induced in (11) is directly proportional to the rotation speed of the shaft and can be expressed more easily with EMF constant k_{emf} as in (12) [11]. Thus, the peak value of the induced back EMF force can be written as in (13).

$$k_{emf} = \sqrt{3}\frac{p}{2}N_t\bar{B}_g A_g k_{sf} k_w \tag{12}$$

$$\hat{E}_z = k_{emf}\omega_m \tag{13}$$

C. Output Power and Electromagnetic Torque

In PMSMs, the ratio of the output power taken from the shaft to the electrical power supplied to the motor gives efficiency. Therefore, the output power parameter is important in terms of motor characteristics [1]. The expression of motor output power is given in (14) in watts [11]. E_z represents the rms value ($\hat{E}_z/\sqrt{2}$) of the EMF per phase, and I represents the phase rms current. This statement is valid in vector control mode in which the air gap flux created by the magnets does not change, only the q-axis current is excited [11].

$$P = 3E_zI \tag{14}$$

The torque expression which is produced by depending on the output power and the angular velocity (rad/s) on the

output shaft is expressed as in (15). It can be written more clearly using the previous equations as in (16). The torque constant k_t value is obtained from this equation as in (17). As it can be clearly seen from (17), the output torque in the motor shaft is directly proportional to I, which is the rms value of the phase current, and the output torque does not change unless the field excitation current changes. Torque, power and current values in these equations are all rated values written on the motor label [1].

$$_R = \frac{P}{\omega_m} \tag{15}$$

$$_R = 3\frac{1}{\sqrt{2}}\frac{p}{2}N_t\bar{B}_g A_g k_{sf} k_w I \tag{16}$$

$$k_t = 3\frac{1}{\sqrt{2}}\frac{p}{2}N_t\bar{B}_g A_g k_{sf} k_w \tag{17}$$

D. Dimensions of PMSM

Geometric dimensions of the inner rotor PMSM are shared in Fig. 2.

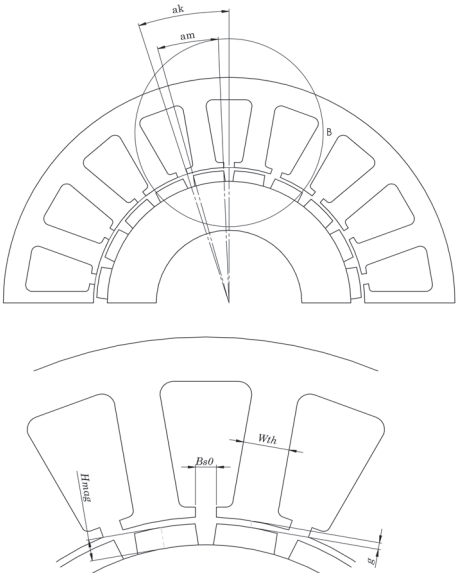

Fig. 2. Dimensions of PMSM

One of the most important parameters to obtain a high performance motor is the slot/pole ratio. While determining this ratio, it should be taken into consideration that there are no unbalanced magnetic forces. When the number of slots per pole per phase value q presented in (18) is not selected correctly, significant unbalanced magnetic forces arise due to the asymmetric placement of slots and windings [13]. N_{slot} in the equation indicates the number of slots, p indicates the number of poles, and n_f indicates the number of phases.

$$q = \frac{N_{slot}}{p \cdot n_f} \tag{18}$$

If the number of slots per pole per phase in a motor is less than 1, these types of motors are called fractional slot winding motors. Designs with q value between 1/2 and 1/3 generally produce high performance, have low cogging torque and high winding factor values [14]. In the study, an 18-slot 20-pole motor design with q value of 0.375 and winding factor of 0.945 has been selected to meet the desired properties.

III. FEM ANALYSIS OF PMSM

First of all, studies related to the stator outer diameter, rotor outer diameter and stack lengths of the motor were carried out. Then the design studies have been continued considering the parameters such as air gap, slot-pole ratio, slot shapes, stator tooth structure, magnet embrace, magnet thickness, wire size, etc. As a result of the optimization studies carried out, the final design has been achieved in the limits of current densities.

The optimization of parameters such as the slot opening (*Bs0*), magnet thickness (*Hmag*), embrace (*Em*), stator tooth thickness (*Wth*) and air gap (*g*) was carried out by using 2D FEM analysis via genetic algorithm. These parameters directly affect the motor efficiency and torque ripples.

The optimization conditions are determined as in Table 1. In this way; after reaching the nominal speed of the motor, the efficiency target value was determined as 90.5% and above, and the torque ripple target value was determined as 0.4 (SI) and below.

TABLE I. OPTIMIZATION CONDITIONS

Optimizer	Calculation	Calculation Time	Condition	Goal
Genetic Algotithm	Efficiency	0.12s-0.2s	>=	90.5%
	Torque Ripple	0.12s-0.2s	<=	0.4 (SI)

A. Optimization Data of PMSM with 18-Slot 20-Pole

The values of slot opening (*Bs0*) 3-6 mm, magnet thickness (*Hmag*) 3.5-5 mm, embrace (*Em*) 0.7-0.9, stator tooth thickness (*Wth*) 10-11mm and motor air gap (*g*) 0.6-1 mm were selected as limit values during the optimization by genetic algorithm.The optimization data set-limits of PMSM with 18-slot 20-pole are given in Table 2.

TABLE II. OPTIMIZATION DATA OF 18-SLOT 20-POLE PMSM

Variable	Starting	Min	Max	Optimizer	Unit
Bs0	5	3	6	4.7549	mm
Em	0.8	0.7	0.9	0.7398	-
Hmag	4	3.5	5	4.8148	mm
g	1	0,6	1,2	0.7609	mm
Wth	10.5	10	11	10.61	mm

B. Optizimation Results of PSMS

In the optimization calculations, motor efficiency reached the targeted limit 90.5% and the torque ripple value was obtained below 0.4 (SI). Efficiency-torque ripple optimization results are shown in Fig 3. The highest efficiency near the limit point of torque ripple was selected. Therefore, the values were obtained where *Bs0* was 4.7549, *Em* was 0.7398, *Hmag* was 4.8148, *g* was 0.7609 and *Wth* was 10.61. Accordingly, it is found the efficiency was 90.63% and the torque ripple was 0.37 (SI).

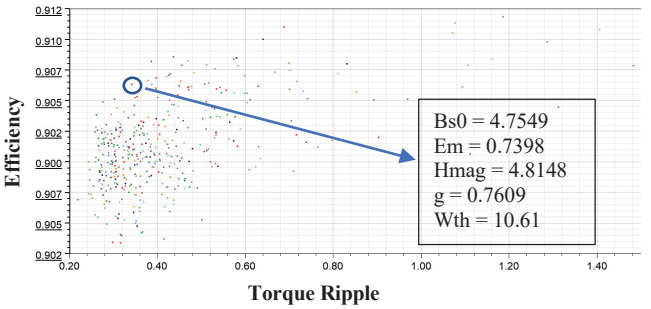

Fig. 3. Efficiency-torque ripple optimization results

C. Design Results

After basic dimensioning of the PMSM, the results were obtained according to the analytical model, then the Ansys RMxprt and 2D FEM genetic algorithm optimization analysis. These results are shown in Table 3. The best results have been obtained in the 2D FEM optimization study made with genetic algorithm.

TABLE III. COMPARISON OF RESULTS

Parameter	Analytical	2D FEM	Unit
Output power (P_{out})	4500	4500	Watt
Input power (P_{in})	4988	4965	Watt
Voltage (V)	380	380	Volt
Phase current (I)	8.1	8.03	Amper
Iron losses (P_{iron})	99	86	Watt
Copper losses (P_{copper})	356	346	Watt
Other losser (P_{other})	33	33	Watt
Efficiency (η)	90.22	90.63	%
Slot fill factor	72	72	%
Current density (J)	5.73	5.9	A/mm^2
Phase resistance (R_s)	1.81	1.78	Ω
Cos φ	0.935	0.94	-

Some transient analysis graphs of the final model obtained from 2D FEM genetic algorithm optimization are shared in Fig. 4-9. Also the PMSM parameters are shown in Table 4.

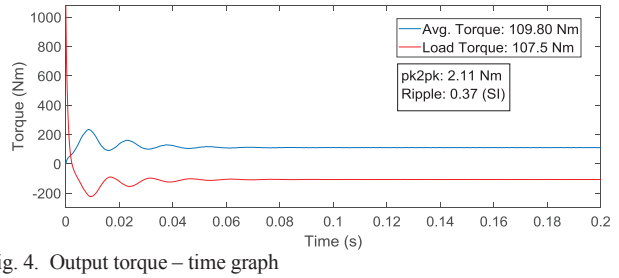

Fig. 4. Output torque – time graph

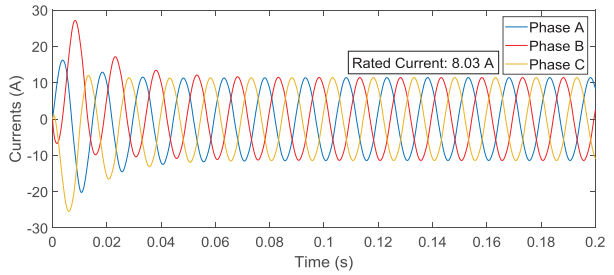

Fig. 5. Phase current-time graph

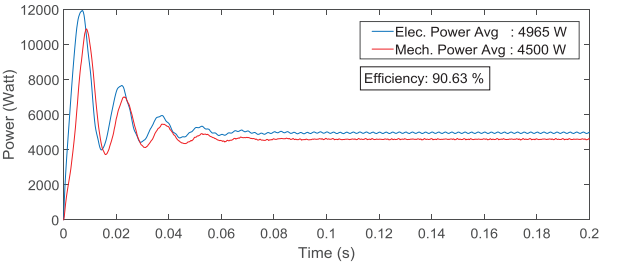

Fig. 6. Input power – output power graph

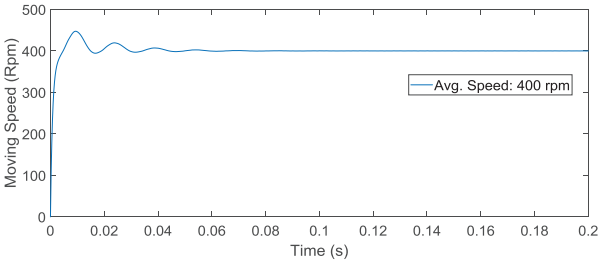

Fig. 7. Motor speed- time graph

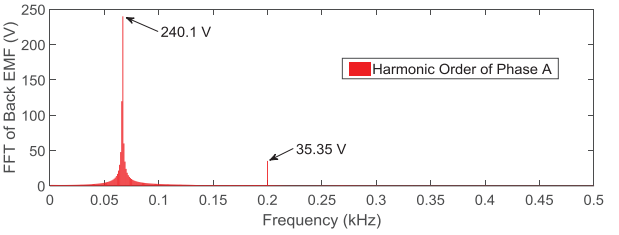

Fig. 8. Harmonic order

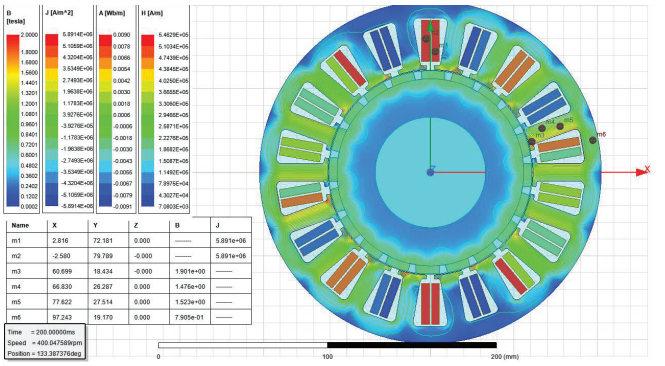

Fig. 9. Magnetic flux density (Tesla), electric current density (A/m^2), magnetic vector potential (Wb/m) and magnetic field strength (A/m)

TABLE IV. MOTOR PARAMETERS

	Parameter	Value	Unit
Motor Feature	Rotor type	Inner rotor	-
	Pole number, p	20	-
	Output power, P	4500	W
	Frequence, f	66.66	Hz
	Voltage, V	380	V
	Rated speed, ω_m	400	rpm
	Rated current, I	8.03	A (rms)
	Rated torque, T_R	107.5	Nm
	Slot number, N_{slot}	18	-
	Rotor material	JFE-400JN50A	-
	Air gap length, g	0.7609	mm
	Magnet thickness, h_{mag}	4.81	mm

Magnet	Magnet type	N45SH	-
	Permeability, μ_r	1.05	-
	Remanence, B_r	1.35	T
	Embrace, *Em*	0.7398	-
Windings	Circuit type	Y	-
	Winding type	concentric	-
	Layer	2	-
Stator	Stacking factor, k_{sf}	0.95	-
	Stator material	JFE-400JN50A	-
	Winding factor, k_w	0.945	-
	Slot opening, B_{s0}	4.7549	mm

Fig. 4 shows the load torque and average output torque of the PMSM. Pick to pick torque ripple is 2.11 Nm and it is 1.92% of the output torque. The rated phase current and inrush current was obtained from Fig. 5 as 8.03 A and 27.13 A respectively. Input power (electrical power) and output power (mechanical power) of the designed PMSM were 4965 W and 4500 W respectively and so the efficiency was obtained 90.63%. in Fig. 6. The PMSM has a rated speed of 400 rpm and reaches steady state speed in approximately 0.08 seconds. Also there is no fluctuation in the speed-time curve as shown in Fig. 7. The 3rd harmonic is achieved 35.35 V from Fig. 8 and there are no other harmonics. In Fig. 9, the electric current density in the windings is about 5.89 A/m^2 and the magnetic flux density in the teeth of stator is about 1.52 Tesla, which is acceptable for PMSMs that have no cooling systems [15, 16].

IV. Conclusion

In this study, the analytical and 2D FEM analysis of a PMSM with 4.5 kW power, 400 rpm speed, 630 kg load capacity were performed in order to be used in belt drive elevator systems. For achieving the optimum PMSM, optimization of the parameters such as the slot opening (*Bs0*), magnet thickness (*Hmag*), embrace (*Em*), stator tooth thickness (*Wth*) and air gap (*g*) was carried out with 2D FEM analysis via using genetic algorithm. 473 different solutions was made. As a result, a PMSM was designed with 18/20 slot-pole ratio, 90.63% efficiency and 0.37 (SI) torque ripple. Results of the transient analysis and detailed parameters of the PMSM were presented. Finally, a high efficiency IE4 class motor with low torque ripple which can be used in belt drive elevator systems was obtained. Future studies will be related to prototype production and real-time testing of PMSM, which will be based on optimization results.

Acknowledgment

This study has been supported by Scientific Research Projects Unit of Tokat Gaziosmanpasa University with the project number of 2021/02.

References

[1] Soyaslan, M. (2020). Design of an External Rotor Permanent Magnet Synchronous Motor for Elevator Traction Systems, PhD Thesis. Sakarya University, Institute of Natural Sciences, Sakarya.

[2] Duru, H.T., Demiröz, R., Toktaş, Y. (2005). Asansör Sistemlerinde Doğrudan Tahrik ve Mıknatıs Uyarmalı Senkron Motor Kullanılarak Enerji Verimliğilinin Yükseltilmesi, I. Enerji Verimliliği ve Kalitesi Sempozyumu, Kocaeli.

[3] Küçükçalık, M. M. (2016). Asansörlerde Enerji Sınıflandırılması ve Verimliliği Artırmak İçin Alınabilecek Tedbirler, Asansör Sempozyumu, İzmir.

[4] Demiröz, R., Saroğlu, S., & Yaprak, H. (2015). Kayış Tahrikli Asansör Sisteminin Tasarımı Ve Uygulanması. 6. Enerji Verimliliği, Kalitesi Sempozyumu ve Sergisi, Kocaeli.

[5] Soyaslan, M., Avşar, Y., Fenercioğlu, A. & Eldoğan, O. (2021). Asansörlerde Kullanilan Dıştan Rotorlu Bir Tahrik Motoru, Turk Patent No. 2021/004176.

[6] Cho, D. H., Kim, J. K., Jung, H. K., & Lee, C. G. (2003). Optimal design of permanent-magnet motor using autotuning niching genetic algorithm. IEEE Transactions on Magnetics, 39(3), 1265-1268.

[7] Sooriyakumar, G., Perryman, R., & Dodds, S. J. (2010). Design optimisation for permanent magnet synchronous motors using genetic algorithm. IEEE 45th International Universities Power Engineering Conference UPEC2010 (pp. 1-6).

[8] Heikkila, T. (2002). Permanent Magnet Synchronous Motor For Industrial Inverter Applications, Analysis And Design (PhD thesis). Lappeenranta University of Technology, Graduate School of Electrical Engineering, Lappeenranta.

[9] Soyaslan, M., Avşar, Y., Fenercioğlu, A. & Eldoğan, O. (2019). Cogging Torque Reduction in External Rotor PM Synchronous Motors by Optimum Pole Embrace. IEEE 3rd International Symposium on Multidisciplinary Studies and Innovative Technologies (ISMSIT), Ankara.

[10] Hanselman, D. C. (2003). Brushless permanent magnet motor design. 2nd Edition, The Writers' Collective.

[11] Şahin, İ. (2010). Measurement Of Brushless DC Motor Characteristics and Parameters and Brushless DC Motor Design, Master's Thesis. Middle East Technical University, The Graduate School of Natural and Applied Sciences, Ankara.

[12] Çağan, N. (2015). Desıgn of an Outer-Rotor Brushless DC Motor For Control Moment Gyroscope Applications (Master's Thesis). Middle East Technical University, The Graduate School of Natural and Applied Sciences, Ankara.

[13] Tanç, G. (2014). Design and implementation of brushless dc motor for electric bicycles, Master's Thesis. Istanbul Technical University, Institute of Natural Sciences, Istanbul.

[14] Salminen, P. (2004). Fractional Slot Permanent Magnet Synchronous Motors For Low Speed Applications, PhD Thesis. Lappeenranta University of Technology, Department of Electrical Engineering, Lappeenranta.

[15] Lipo, T. A. (2017). Introduction to AC Machine Design. IEEE Press, John Wiley & Sons.

[16] Pyrhonen, J., Jokinen, T., & Hrabovcova, V. (2013). Design of rotating electrical machines. John Wiley & Sons.